Roles of P-body factors in *Candida albicans* filamentation and stress response

Melissa A. Tosiano[1], Frederick Lanni[1], Aaron P. Mitchell[2], C. Joel McManus[1]*

1 Department of Biological Sciences, Carnegie Mellon University, Pittsburgh, Pennsylvania, United States of America, **2** Department of Microbiology, University of Georgia, Athens, Georgia, United States of America

*Corresponding author

mcmanus@andrew.cmu.edu

Abstract

Hyphal growth is strongly associated with virulence in the human fungal pathogen *Candida albicans*. While hyphal transcriptional networks have been the subject of intense study, relatively little is known about post-transcriptional regulation. Previous work reported that P Body (PB) factors Dhh1 and Edc3 were required for virulence and filamentation, suggesting an essential role for post-transcriptional regulation of these processes. However, the molecular roles of these factors have not been determined. To further study the function of PB factors in filamentation, we generated homozygous deletions of *DHH1* and *EDC3* in the prototrophic strain SC5314 using CRISPR-Cas9. Homozygous *dhh1* deletion strongly impaired growth and altered filamentation, in addition to exhibiting unusual colony morphology in response to heat stress. Using RNA-seq, we found *DHH1* deletion disrupts the regulation of thousands of genes under both yeast and hyphal growth conditions. This included upregulation of many stress response genes in the absence of stress, similar to deletion of the *S. cerevisiae DHH1* homolog. In

contrast, we found *EDC3* was not required for heat tolerance or filamentation. These results support a model in which *DHH1*, but not *EDC3*, represses hyphal stress response transcripts in yeast and remodels the transcriptome during filamentation. Our paper supports distinct requirements for specific mRNA decay factors, bolstering evidence for post-transcriptional regulation of filamentation in *C. albicans*.

Author summary

In the dimorphic fungal pathogen *C. albicans*, the hyphal phenotype corresponds with pathogenicity. While transcriptional control of hyphal growth has been extensively studied, comparatively little is known about post-transcriptional regulation of this significant morphological shift. PB factors are associated with mRNA decay and translational repression. Here we investigate the roles of two PB factors in growth, filamentation, and gene expression. Although deletion of PB factor EDC3 did not impact growth or filamentation, *dhh1Δ/Δ* had greatly impaired growth and heat tolerance as well as unusual hyphal phenotypes. Additionally, we found that the transcriptomes of *dhh1Δ/Δ* yeast and hyphae were highly dysregulated. The extensive transcriptomic impacts of the absence of Dhh1 correlated with our phenotypic findings. Stress-associated genes were induced under non-stress conditions and the filamentation response was blunted under physiologically relevant *in vitro* conditions. We demonstrate that mRNA decay factors play distinct roles in regulating *C. albicans* morphology and that Dhh1 contributes to environmentally appropriate expression of the stress response and hyphal growth.

Introduction

43 *Candida albicans* lives as a commensal organism in immunocompetent humans [1]. However,
44 this opportunistic fungus causes blood and deep tissue infections (candidiasis) in
45 immunocompromised individuals [2]. Pathogenicity requires detecting and responding to stress
46 in divergent physiological microenvironments [3,4]. Under stress, *C. albicans* undergoes the
47 process of filamentation, shifting from commensal yeast to virulent hyphae. Hyphal growth
48 correlates with the release of the peptide toxin candidalysin [5], and adherent biofilm formation
49 [6–8]. Both contribute to pathogenicity. Foundational research on transcriptional regulation of
50 filamentation had identified dozens of transcription factors (TFs) and signaling cascades
51 regulating the core filamentation response networks [9–12]. Under different hyphal-inducing
52 conditions *C. albicans* activates distinct transcriptional programs [13]. Despite deep exploration
53 into transcriptional control of filamentation, comparatively little work has addressed post-
54 transcriptional regulation of filamentation [14,15].

55 Eukaryotes implement swift and precise post-transcriptional stress responses [16,17]
56 appropriate for regulating the acute stage of *C. albicans* filamentation [14,15]. Post-
57 transcriptional regulation of gene expression integrates mRNA translation, localization, and
58 decay [18,19]. Indeed, mRNA decay has been found to regulate adaptation to the host
59 environment and virulence in several human fungal pathogens [3,15,20,21]. Localization to
60 ribonucleoprotein (RNP) granules represses translation and initiates decay in many organisms
61 [22,23]. P-bodies (PBs) are RNPs associated with the Ccr4-not deadenylase complex [23–26]
62 and mRNA degradation [22,23,27]. In *C. albicans*, several PB mRNA decay factors have been
63 reported to function in hyphal development and virulence, including Ccr4, Pop2, Not5, Xrn1,
64 Dhh1, and Edc3 [28–36]. However, the effects of these factors on gene regulation during
65 filamentation have not been elucidated.

66 Stochastic transcriptional noise generates different phenotypic outcomes in clonal microbial
67 populations that serves as a mechanism of “bet-hedging” for acute environmental stressors [37–

68 39]. In this context, mRNA decay provides a system of transcript buffering preventing gene
69 expression under inappropriate conditions [40]. Genes identified as both transcriptionally noisy
70 and poorly translated have these features conserved between *S. cerevisiae* and *C. albicans*
71 homologs [41]. However, the extent to which mRNA decay factors buffer or control noisy
72 expression of hyphal genes under yeast-form conditions or conversely yeast genes under
73 hyphal conditions remains unclear in *C. albicans*. Furthermore, the roles of *C. albicans* PB
74 factors in buffering noisy transcription for environmentally appropriate gene expression have not
75 been elucidated.

76 In the model yeast *S. cerevisiae*, the functions of PB factors Dhh1 and Edc3 have been
77 extensively studied [42]. The DEAD-box helicase and activator of mRNA decapping Dhh1
78 rapidly exchanges between the cytoplasm and PBs [43,44]. It has been proposed that Dhh1
79 integrates translation and mRNA decay by interacting with ribosomes to repress translation and
80 stimulating the decay of slow translating mRNA with poor codon optimality [45,46]. Contrary to
81 this, it has been reported that Dhh1 does not recognize targets for decay by slow translation or
82 codon optimality. Instead, Dhh1 represses genes associated with nutrient limitation, cell wall
83 components, autophagy, and metabolism of non-preferred carbon and nitrogen sources under
84 optimal growth conditions [47]. Interestingly, Dhh1 has also been reported to induce translation
85 in mRNA with structures in the coding sequence approximately 70 nucleotides downstream from
86 the translation initiation site [48]. Loss of *DHH1* in *S. cerevisiae* downregulates *STE12*
87 translation leading to defects in pseudohyphal growth and mating [34,49,50]. Kinase signaling
88 via Dhh1 phosphorylation sites are critical to pseudohyphal development in *S. cerevisiae*
89 *[34,51]*. Our other PB factor of interest, Edc3 acts as a non-essential enhancer of mRNA
90 decapping and PB scaffolding factor [42,43,52]. In *S. cerevisiae*, absence of Edc3 reduces PB
91 assembly size, but does not impede global mRNA decay [43,53]. Additionally, Edc3 is also
92 dispensable for PB formation in *S. pombe* [54]. In contrast to *S. cerevisiae*, the roles of Dhh1

93 and Edc3 in *C. albicans* hyphal growth have been minimally explored and the function of Dhh1
94 on gene expression remains unknown in this species.

95 Prior work in *C. albicans* reported that both Dhh1 and Edc3 are necessary for WT stress
96 tolerance and filamentation. In a *C. albicans* auxotrophic background, the authors described a
97 heterozygous deletion of *DHH1* (*DHH1/dhh1Δ*) which produced WT colonies on YPD plates, but
98 was filamentation impaired [34]. In the same *C. albicans* auxotrophic background, *edc3Δ/Δ* was
99 noted to have impaired PB condensation, reduced heat tolerance at 37°C, and severely
100 restricted filamentation [35,36]. This early research implied that *DHH1* and *EDC3* may have
101 distinct roles in *C. albicans* filamentation. However, the gene regulatory effects of *DHH1*
102 deletion in *C. albicans* have not been defined. Thus, our understanding of these important PB
103 factors in filamentation remains limited.

104 In this study, we investigated the roles of PB factor Dhh1 in *C. albicans* heat tolerance,
105 filamentation, and gene expression. Using transient CRISPR-cas9 [55] we deleted *DHH1* and
106 *EDC3* in SC5314. We demonstrated the dispensability of *EDC3* for PB condensation, heat
107 tolerance, and filamentation. Importantly, we found *dhh1Δ/Δ* exhibits impaired yeast-form
108 growth, heat sensitivity, and anomalous filamentation. Finally, we determined the effects of
109 *dhh1Δ/Δ* on gene expression genome wide in yeast and early hyphae, and found loss of *DHH1*
110 causes widespread dysregulation of the transcriptome and stress responses.

111 Results

112

113 Characterizing P-Bodies (PBs) in *C. albicans*

114 To investigate the presence of dhh1 and edc3 in PBs, we first generated prototrophic strains
115 with fluorescently labeled PB factors. We fused mScarlet to the C-terminus of Dhh1 (Dhh1-mS)

116 and mNeonGreen to the C-terminus of Edc3 (Edc3-mNG) using CRISPR-Cas mediated
117 genome editing. During acute heat shock Edc3-mNG condensed into round foci (Fig 1. A). To
118 determine if these foci were PBs, we generated a dual labeled strain (Edc3-mNG, Dhh1-mS)
119 and exposed it to identical heat shock conditions. Edc3-mNG and Dhh1-mS colocalized,
120 confirming these foci were PBs (Fig 1. B). In *S. cerevisiae* Edc3 is more stably associated with
121 PBs than Dhh1, which rapidly exchanges with the cytoplasm [56]. Similarly, we found a large
122 fraction of Dhh1 was cytoplasmically diffuse, suggesting Dhh1 functions both in PBs and in the
123 cytoplasm (Fig 1. B). We next investigated PB condensation during early filamentation. After 3
124 hours of acute glucose starvation, PBs were abundant in yeast cells and along developing
125 hyphal germ tubes (Fig 1. C). Lastly, we investigated whether these proteins were
126 independently required for PB condensation. In the absence of Edc3, Dhh1-mS retained the
127 capacity to form condensates in response to acute heat shock (Fig 1. D). Similarly, Edc3-mNG
128 also condensed in the absence of Dhh1 (Fig 1. E). In summary, we confirmed the presence of
129 PBs in stressed *C. albicans* and found that, as in *S. cerevisiae*, *C. albicans* PBs are robust
130 condensates that can tolerate the absence of Dhh1 or Edc3 individually.

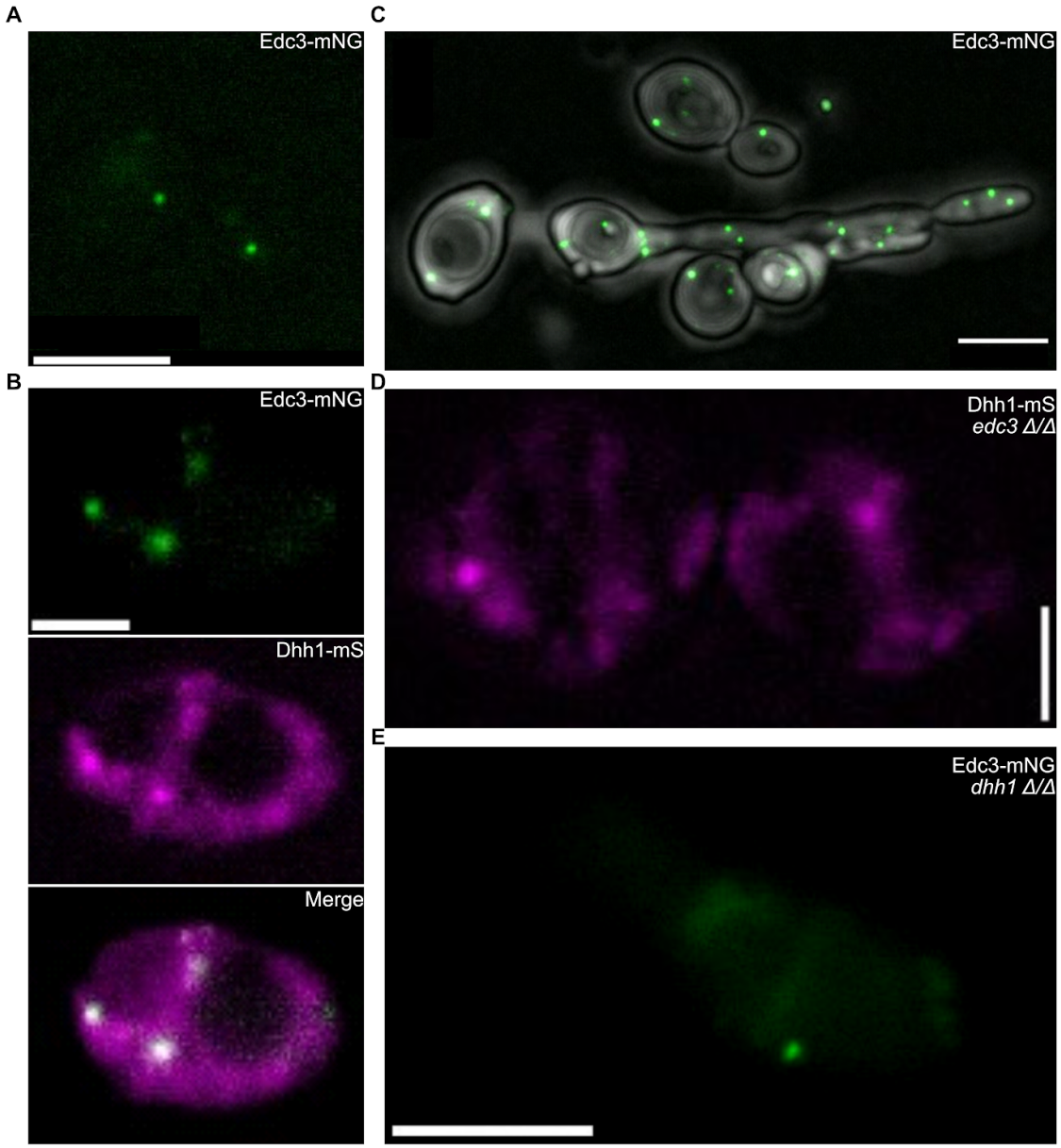

Fig 1. PBs condense during acute stress. Fluorescent and confocal images of SC5314 PB factors fluorescently tagged within the genome. **A.** Edc3-mNG condensed in live *C. albicans* SC5314 in response to acute heat shock (10m at 46°C). Scale bar = 5μm. **B.** PB factors (Edc3-mNG and DHH1-mS) co-localized during acute heat shock and confirmed their identity as PBs. Scale bar = 2μm. **C.** 3-hours of starvation generated abundant PBs (Edc3-mNG) along the

137 developing germ tube. Scale bar = 5μm. **D.** Dhh1-mS condensed in the absence of Edc3. Scale
138 bar = 2μm. **E.** Edc3-mNG condensed in the absence of Dhh1. Scale bar = 5μm.

139 *DHH1* is required for normal growth and stress response
140 phenotypes

141 We next investigated the role of Dhh1 and Edc3 in *C. albicans* growth and stress responses.
142 We generated heterozygous (*DHH1*/*dhh1Δ*) and homozygous (*dhh1Δ/Δ*) *DHH1* deletions and
143 complements in SC5314. We initially conducted spot assays at 30°C and 37°C to test for growth
144 and temperature sensitivity defects. We found strains possessing at least one copy of *DHH1*
145 produced colonies identical to WT on YPD plates (Fig 2. A-B). However, *dhh1Δ/Δ* had inhibited
146 growth across timepoints and incubation temperatures (Fig 2. A-B). Uniquely, after 3 days at
147 37°C, *dhh1Δ/Δ* colonies also exhibited a wrinkled appearance associated with hyphal growth
148 (Fig 2. B). To further investigate this phenomenon, we grew colonies at 37°C for 4 days on YPD.
149 While all strains with *DHH1* had a smooth surface and soft texture, *dhh1Δ/Δ* colonies had a
150 wrinkled surface and firm, dry texture (Fig 2. C). *dhh1Δ/Δ* grew more slowly than WT and
151 complement strains at 30°C in liquid YPD (Fig 3. A). Surprisingly, DIC microscopy revealed
152 *dhh1Δ/Δ* cells were nearly twice the size of the *DHH1* containing strains, with enlarged vacuoles
153 (Fig 3. B). The slow growth and altered cell physiology of *dhh1Δ/Δ* suggested the induction of
154 stress associated phenotypes in the absence of environmental stressors. In contrast, the loss of
155 *EDC3* did not impair spot assay growth at 30°C and 37°C (Fig S1. A). Thus, we focused the
156 remainder of this study on *DHH1*.

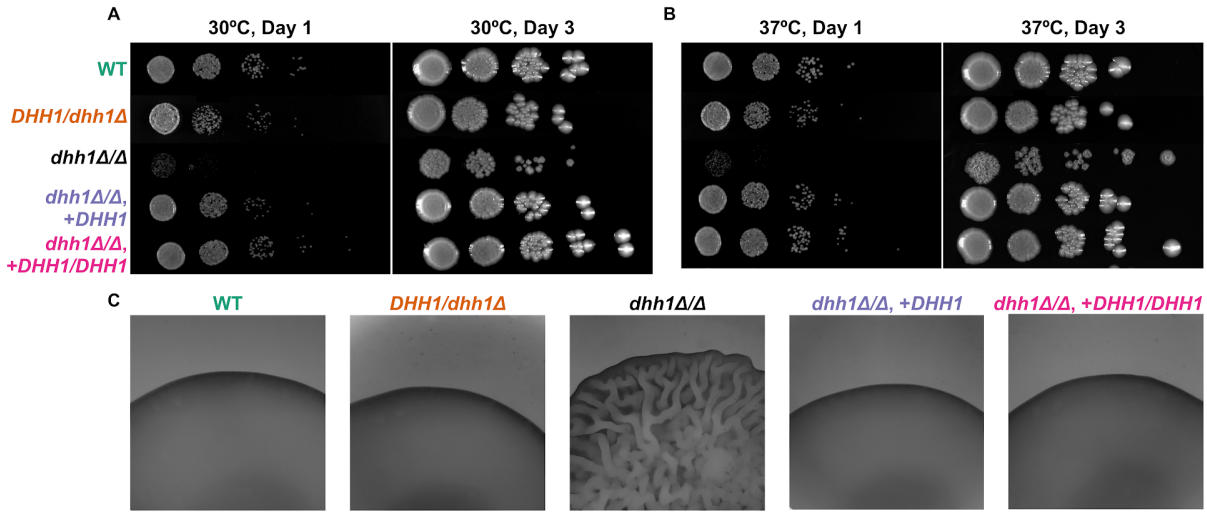

Fig 2. In SC5314, *DHH1* is required for WT colony growth and morphology. In all of the strains, at least one copy of *DHH1* was needed for WT growth and colony phenotype. Only *dhh1Δ/Δ* displayed growth impairment and pseudohyphal colonies in response to heat stress. **A.** Day 1 and 3 of a 30°C spot plate assay of WT and mutant SC5314. **B.** Day 1 and 3 of a 37°C spot plate assay of WT and mutants SC5314. **C.** Colonies after 4 days of incubation on YPD at 37°C. 25X magnification.

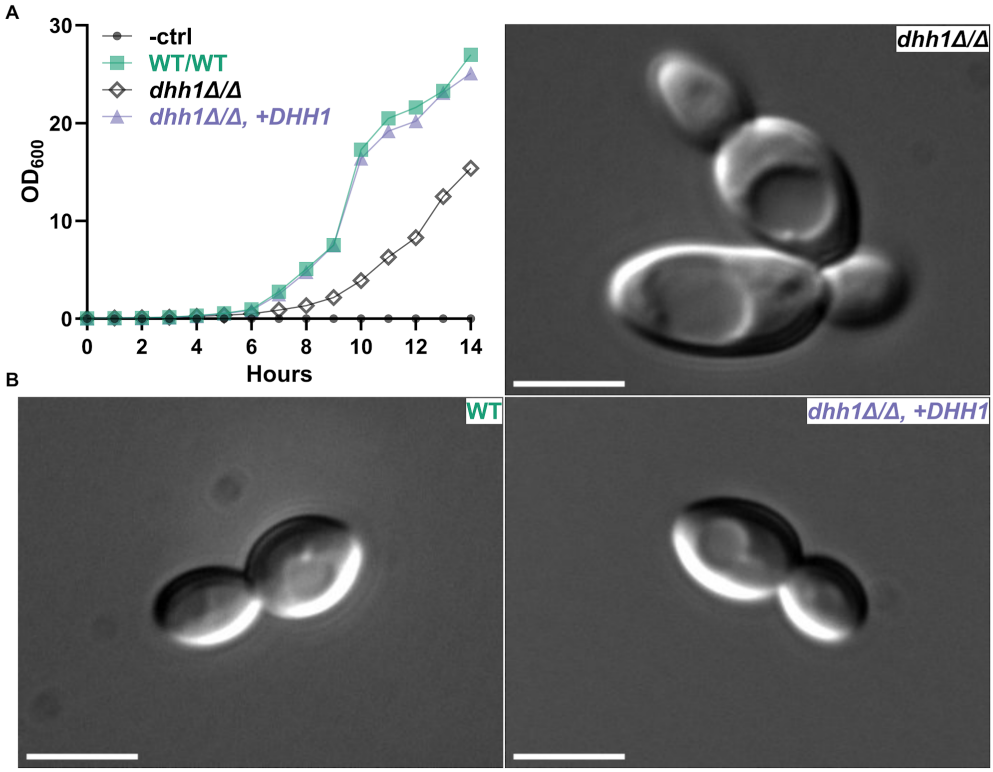

Fig 3. Absence of *DHH1* alters growth and cell physiology. WT and mutant strains were grown in liquid YPD with shaking at 30°C over 14 hours. **A.** Exponential growth was impaired in *dhh1Δ/Δ* and rescued by the complement (*dhh1Δ/Δ, +DHH1*). **B.** DIC images of exponentially growing cells show enlarged cell bodies and vacuoles in *dhh1Δ/Δ*. Scale bar = 5μm.

DHH1 is necessary for WT filamentation

Considering the aberrant phenotypes of *dhh1Δ/Δ* in rich media, we next examined the possibility of accompanying filamentation defects. *dhh1Δ/Δ* cells were larger than WT and complement strains after 4 hours of filamentation, with the cell body taking up a greater proportion of the total length -(Fig 4. A). However, the median length to width ratio of *dhh1Δ/Δ* cells was significantly smaller -(Fig 4. B). After 16 hours of planktonic filamentation, *dhh1Δ/Δ* cells remained enlarged with thick curved germ tubes and fewer septa compared to WT and complement strains (Fig 4. C). The median length to width ratio of *dhh1Δ/Δ* at 16 hours was also significantly less than the

177 other strains (Fig 4. D). In summary, we found that a single copy of *DHH1* sufficiently supported
178 WT planktonic filamentation, while homozygous deletion resulted in abnormal filamentous
179 growth at both timepoints.

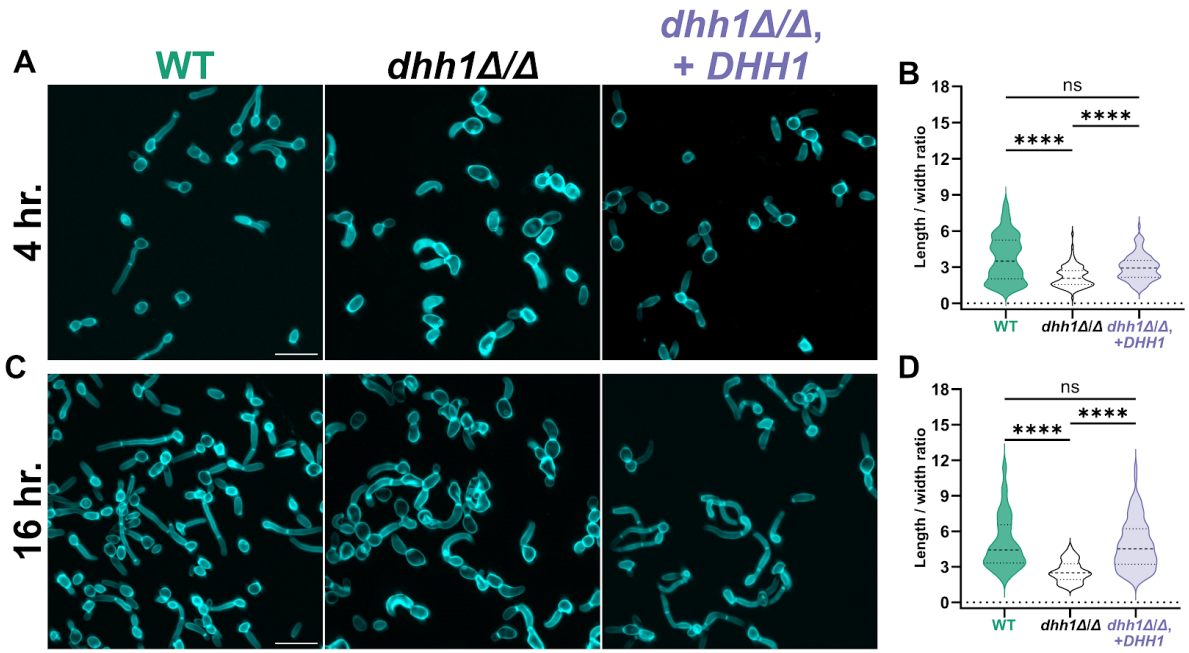

180

181 **Fig 4. *DHH1* is required for WT planktonic filamentation.** WT and mutant strains grown
182 under physiologically relevant filamentation conditions. (37°C, RPMI + 10% FBS). **A.** Strains
183 were subjected to a planktonic 4-hour filamentation assay. Scale bar = 20μm. **B.** After 4-hours
184 of filamentation, *dhh1Δ/Δ* had less developed germ tubes defined as length by width of 100 cells
185 in at least 4 fields of view. (Kruskal-Wallis test for significant variance of median. ****P <
186 0.0001). **C.** Strains were subjected to a planktonic 16-hour filamentation assay. Scale bar =
187 20μm. **D.** After 16-hours of filamentation, *dhh1Δ/Δ* had less developed germ tubes defined as
188 length by width of 100 cells in at least 4 fields of view (Kruskal-Wallis test for significant variance
189 of median. ****P < 0.0001).

190 Due to the significant impairment of planktonic filamentation in *dhh1Δ/Δ,* we expected *dhh1Δ/Δ*
191 to exhibit comparatively short defective biofilms. Surprisingly, *dhh1Δ/Δ* generated deep, diffuse

192 biofilms compared to WT and complement strains (Fig 5. A & B). Nevertheless, *dhh1Δ/Δ*
193 biofilms exhibited other key differences. In WT and *DHH1* complement strains, cells were
194 concentrated near the base of the biofilm (Fig 5. C). Using pixel intensity as a proxy for cell
195 density, we quantitatively demonstrated that *dhh1Δ/Δ* biofilm architecture was altered with a
196 maximum cell density further removed from the basal layer of the biofilm compared to WT and
197 *DHH1* complement (Fig 5. D). This altered biofilm structure may result from the somewhat
198 hyperfilamentous *dhh1Δ/Δ* strain, via decreased yeast cell proliferation at the base of the
199 structure.

200 Next, we surveyed the phenotype of colonies during invasive growth on spider media. After 6
201 days of growth, *dhh1Δ/Δ* colonies revealed a wrinkled hyphal phenotype but a marked absence
202 of hyperfilamentous margins found in WT SC5314 (Fig 5. E). Compared to other strains,
203 *dhh1Δ/Δ* colonies grew more vertically with tighter wrinkles (Fig 5. E). Again as in the other
204 filamentation assays, our complement strain with a single *DHH1* copy produced WT colonies on
205 spider media (Fig 5. E). Furthermore, in contrast to *dhh1Δ/Δ, edc3Δ/Δ* was indistinguishable
206 from WT in all 3 filamentation assays (Fig S1. B-F). In conclusion *dhh1Δ/Δ* failed to generate
207 WT germ tubes, biofilm composition or invasive colonies on spider media supporting a role for
208 this RNA decay factor in filamentation.

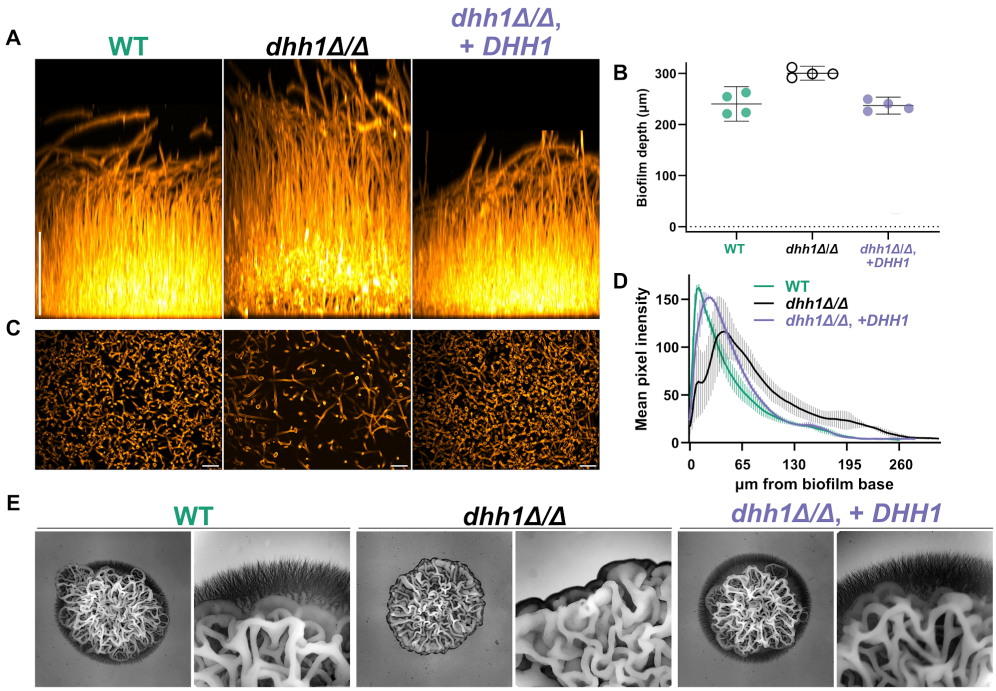

Fig 5. Absence of *DHH1* alters biofilm and spider colony morphology. WT and mutant strains grown in two *in vitro* filamentation assays. **A.** Side-view of WT and mutant strains after a 24-hour biofilm assay. (37°C, RPMI + 10% FBS). Scale bar = 100µm. **B.** Depth of 4 replicate biofilms. CI = 95%. **C.** Basal views 26µm from the bottom of the biofilm showed a lower concentration of *dhh1Δ/Δ* cells. Scale bar = 20µm. **D.** Pixel intensity from 4 replicate biofilms (SD) varied with biofilm depth. Strains with at least one copy of *DHH1* had a greater concentration of cells closer to the base of the biofilm than *dhh1Δ/Δ* based on brightness. **E.** Colonies grown on spider plates (37°C). 6X and 25X magnification.

Loss of DHH1 disrupts numerous pathways involved in metabolism and cellular morphology

Given the severe phenotypic defects in both yeast and hyphae that result from *dhh1Δ/Δ*, we next used RNA-seq to identify differentially expressed genes in yeast (30°C, YPD) and early hyphae (37°C, RPMI + 10% FBS, 4 hrs.). In YPD, *dhh1Δ/Δ* yeast had 1,244 genes significantly

223 downregulated and 1,408 genes significantly upregulated ($P < 0.01$) compared to the
224 corresponding wildtype strain (Fig 6. A). Interestingly, *dhh1Δ/Δ* yeast upregulated multiple
225 genes associated with hyphae inducing stress, including *RHR2*, *ECE1*, and *HWP1* (Fig 6. A; Fig
226 S4-5). Indeed, GO terms corresponding to hyphal stress, such as hyphal cell wall and
227 carbohydrate transport, were enriched in genes upregulated in *dhh1Δ/Δ* compared to the WT
228 strain in YPD (Fig 6. B). In RPMI, *dhh1Δ/Δ* hyphae had 1,151 genes downregulated and 1,269
229 genes upregulated ($P < 0.01$) (Fig 6. C). For example, metabolite transport genes were
230 upregulated in *dhh1Δ/Δ* RPMI including *JEN1* and *HGT12* (Fig 6. C). Under RPMI conditions,
231 *dhh1Δ/Δ* inappropriately regulated cell wall genes. Hyphal adhesin *ALS1* was downregulated
232 while yeast cell wall protein *YWP1* was upregulated (Fig 6. C; Fig S6). Genes upregulated in
233 *dhh1Δ/Δ* hyphae were enriched in GO terms related to transport, metabolism and ergosterol
234 biosynthesis (Fig 6. D). While most changes in expression were specific to environmental
235 conditions, there was significant overlap in the genes differentially expressed in *dhh1Δ/Δ* under
236 YPD and RPMI growth conditions (Hypergeometric test, $P < 2.3e^{-22}$; Fig 6. E). Transcription
237 factors regulating morphology were also differentially expressed *dhh1Δ/Δ* in both conditions (Fig
238 6. F). Interestingly, while most TFs shifted in the same direction in both growth conditions,
239 hyphal repressor *NRG1* [57,58] and cell cycle/cell wall stress regulator *SWI6* [59,60] were
240 downregulated in YPD but upregulated in RPMI (Fig 6. E). In summary, our RNA-seq analysis
241 established widespread gene expression aberrations in *dhh1Δ/Δ* yeast and hyphae compared to
242 the parental wildtype strain.

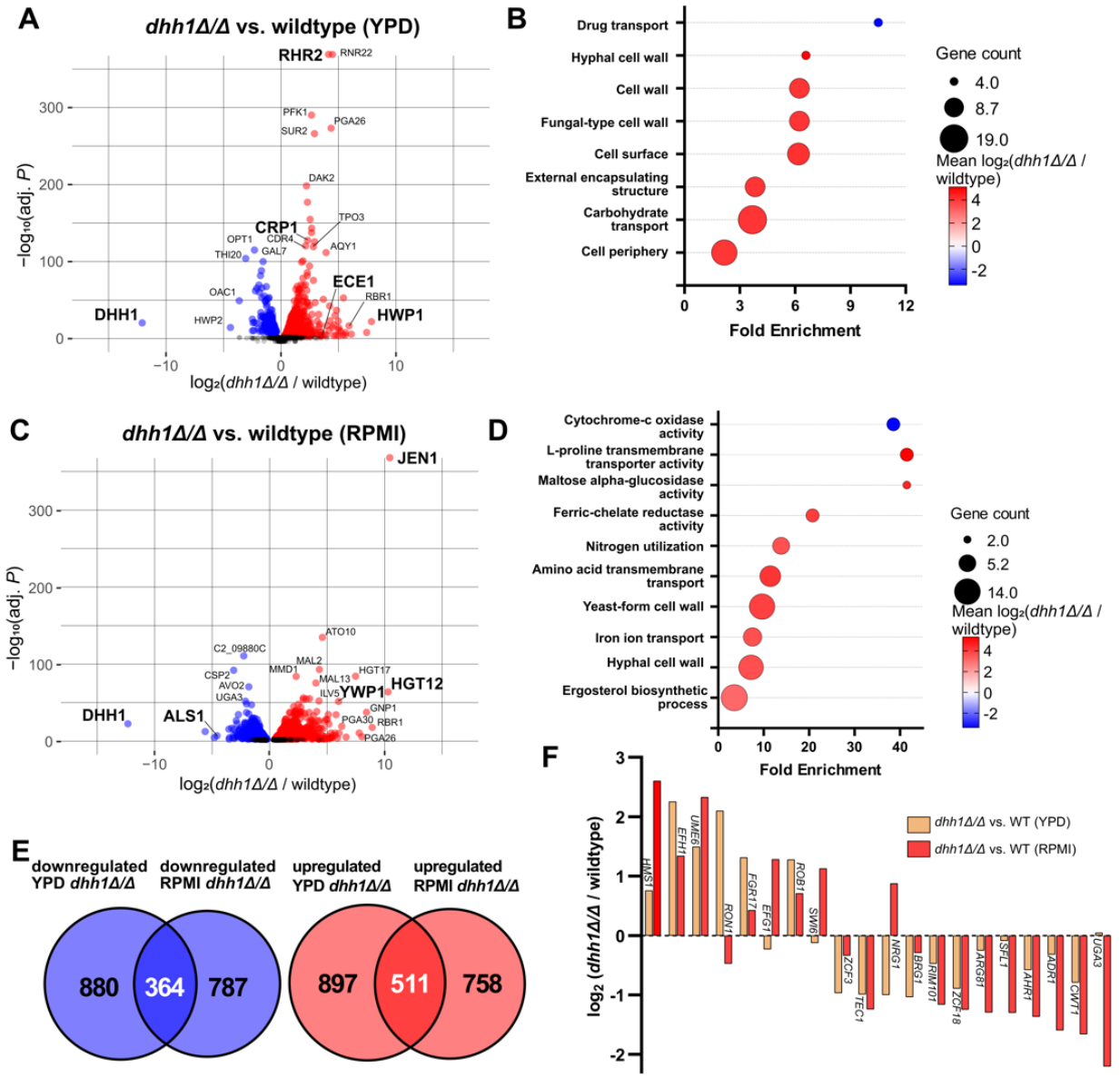

Fig 6. RNA-seq exposed differential gene expression in *dhh1Δ/Δ* grown under YPD and RPMI conditions. A. Volcano plot depicts genes significantly up (red) and down (blue) -regulated during yeast-form growth compared to wildtype. Genes associated with filamentation stress were prominently upregulated (Table S1). **B.** GO terms enriched greater than 2-fold for all genes differentially expressed > 2.5 and <-2.5-fold in *dhh1Δ/Δ* YPD. Transport and cell wall terms were enriched in *dhh1Δ/Δ* YPD. **C.** Volcano plot depicts gene expression differences in *dhh1Δ/Δ* vs wildtype during early hyphal growth (Table S2). Genes associated with metabolite

251 transport and the yeast cell wall were upregulated. **D.** GO terms enriched greater than 2-fold for
252 all genes differentially expressed > 2.5 and <-2.5-fold in *dhh1Δ/Δ* RPMI**.** Transport, cell wall,
253 and metabolic terms were enriched in *dhh1Δ/Δ* RPMI upregulated genes. **E.** A significant
254 number of transcripts were downregulated ($P = 2.28e^{-22}$), and upregulated ($P = 4.37e^{-52}$),
255 respectively, in *dhh1Δ/Δ* in YPD and RPMI conditions. (Hypergeometric test). However, most
256 differentially expressed genes were environmentally specific. **F.** Differential expression of
257 transcription factors regulating morphogenesis in *dhh1Δ/Δ* in YPD and RPMI.

258 Filamentation dependent transcriptome remodeling is
259 reduced in *dhh1Δ/Δ*

260 Our initial analysis of *dhh1Δ/Δ* yielded valuable insights into aberrant gene expression in yeast
261 and hyphae. Several RNA decay mutants are filamentation defective, possibly due to impaired
262 transcriptome remodeling during early filamentation [14,15]. Therefore we next investigated the
263 role of DHH1 in gene regulation during filamentation. Comparing RNA-seq results from the WT
264 strain grown in RPMI to YPD showed the known extensive transcriptome remodeling that occurs
265 during filamentation, with 2,488 downregulated and 2,496 upregulated genes (Fig 7. A, Table
266 S3). Thus, filamentation dramatically restructured the transcriptome in WT *C. albicans*. Hyphal
267 cell wall proteins and ubiquitination factors such as *HWP1* and *BUL1* were upregulated in WT
268 RPMI compared to WT YPD (Fig 7. A). GO terms related to ribosomal RNA, ribosomal proteins,
269 and translation elongation were all -enriched in genes downregulated in WT hyphae, strongly
270 indicating a general reduction in mRNA translation (Fig 7. B). The majority of upregulated GO
271 terms in WT RPMI were enriched in carbohydrate transporters responding to the shift from rich
272 YPD to carbohydrate poor RPMI (Fig 7. C). These results are consistent with known
273 transcriptional changes that occur during filamentation in WT strains [13,61–67].

274 We hypothesized that impaired mRNA decay in *dhh1Δ/Δ* would blunt the downregulation of a
275 subset of genes during filamentation. Indeed, transcriptional remodeling of *dhh1Δ/Δ* was
276 overwhelmingly reduced with 1,795 downregulated and 1,919 upregulated genes, only 75% of
277 the total number of genes remodeled in WT (Fig 7. D). The number of up and downregulated
278 genes during WT filamentation was almost equal with only 8 more genes upregulated compared
279 to downregulated (Fig 7. A). However, *dhh1Δ/Δ* had 124 fewer genes downregulated compared
280 to upregulated, possibly due to impaired mRNA degradation (Fig 7. D). Most of the GO terms
281 enriched in downregulated genes in filamenting *dhh1Δ/Δ* were the same as WT, but with a
282 smaller reduction in mean Log_2(RPMI / YPD) (Fig 7. E). Additionally, in filamenting *dhh1Δ/Δ* the
283 majority of the GO terms enriched in upregulated genes were also present in filamenting WT
284 cells (Fig 7. F). Uniquely, terms related to lipid catabolism were upregulated in *dhh1Δ/Δ* but not
285 WT (Fig 7. C, F). Changes in the expression of morphology related transcription factors were
286 generally less pronounced in *dhh1Δ/Δ* than WT (Fig 7. G). Interestingly, unlike in WT, the
287 filamentation repressor gene *NRG1* was not significantly downregulated in filamenting *dhh1Δ/Δ*,
288 indicating a mechanism for continued repression of select hyphal genes (Fig 7. G). The vast
289 majority of differentially expressed genes in filamenting *dhh1Δ/Δ* were a subset of WT
290 remodeling (Hypergeometric test, P = 0; Fig 7. H). In general, *dhh1Δ/Δ* had a more modest
291 transcriptome remodeling response during filamentation than WT.

292 At 37°C, *dhh1Δ/Δ* colonies on YPD plates have a crinkled morphology similar to WT colonies on
293 spider media (Fig 2. C & Fig 5. E). Thus, we hypothesized that the gene regulatory effects of
294 *dhh1Δ/Δ* in YPD may be similar to the WT filamentation response. We found 44% of genes
295 differentially regulated in *dhh1Δ/Δ under non-stress conditions* (YPD) overlapped with gene
296 expression changes in the filamenting WT strain (Fig 7. I) Notably, there was significant overlap
297 of genes downregulated in both yeast form *dhh1Δ/Δ* and filamenting WT (Hypergeometric test;
298 $P = 2.3e^{-06}$) while the overlap of genes upregulated in both conditions was not significant (P =

0.55). Commonly downregulated genes were associated with metabolic/biosynthetic processes and chromatin. Commonly upregulated genes were involved in carbohydrate transport and autophagy. While the *dhh1Δ/Δ* transcriptome in YPD clearly differs from a wildtype hyphal transcriptome, there was a surprising amount of similarity, suggesting *dhh1Δ/Δ* exhibits some aspects of the WT stress response in a non-stress environment (Fig 8).

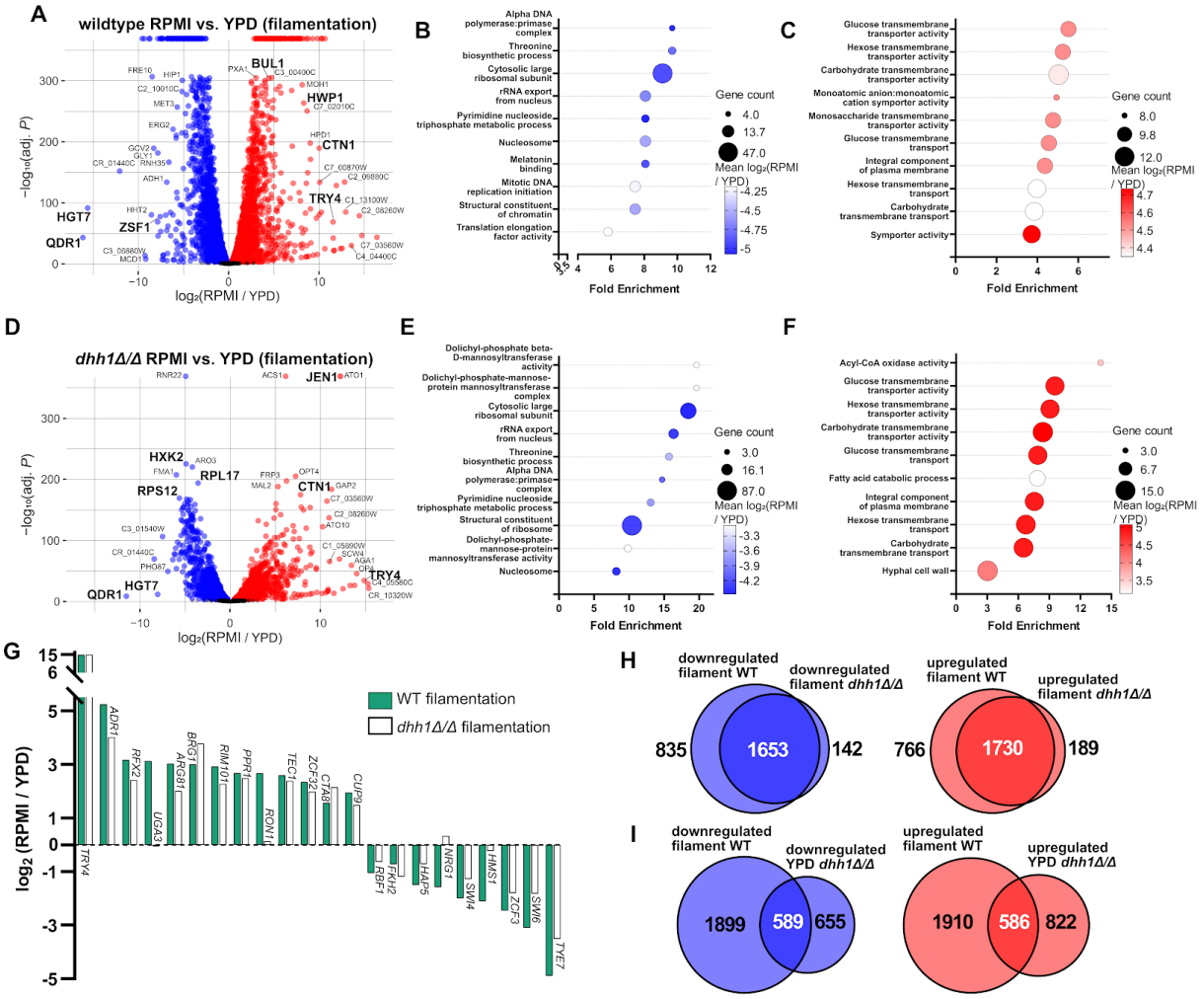

Fig 7. RNA-seq reveals transcriptome differences between WT and *dhh1Δ/Δ* during filamentation. A. Volcano plots comparing the transcriptomes of WT SC5314 grown in YPD and RPMI demonstrate extensive remodeling during filamentation (Table S3). **B.** Expected GO terms were downregulated, and **C.** upregulated during filamentation. **D.** Comparing the

309 transcriptome of *dhh1Δ/Δ* grown in YPD and RPMI showed impaired transcriptome remodeling
310 (Table S4). **E.** Similar GO terms were downregulated, and **F.** upregulated in filamenting
311 *dhh1Δ/Δ* and WT. Unlike WT, *dhh1Δ/Δ* upregulated terms related to lipid catabolism during
312 filamentation. **G.** Transcription factors regulating morphogenesis were differentially expressed
313 during filamentation in WT and *dhh1Δ/Δ*. **H.** Genes differentially expressed during filamentation
314 overlapped between WT and *dhh1Δ/Δ* strains. Most transcripts differentially expressed during
315 *dhh1Δ/Δ* filamentation are subsets of the WT remodeling response. A significant number of
316 transcripts were down- (P = 0) or upregulated (P = 0) in both filamenting *dhh1Δ/Δ* and wild type
317 (Hypergeometric test). **I.** Transcripts that were differentially expressed during WT filamentation
318 and *dhh1Δ/Δ* grown in YPD. Overlapping genes implied that under yeast-form conditions
319 *dhh1Δ/Δ* partially echoed the transcriptome of stressed filamenting cells. Interestingly a
320 significant number of downregulated transcripts (P = $2.3e^{-06}$) were shared between WT
321 filamentation and *dhh1Δ/Δ* YPD, but not upregulated transcripts (P = 0.55). (Hypergeometric
322 test).

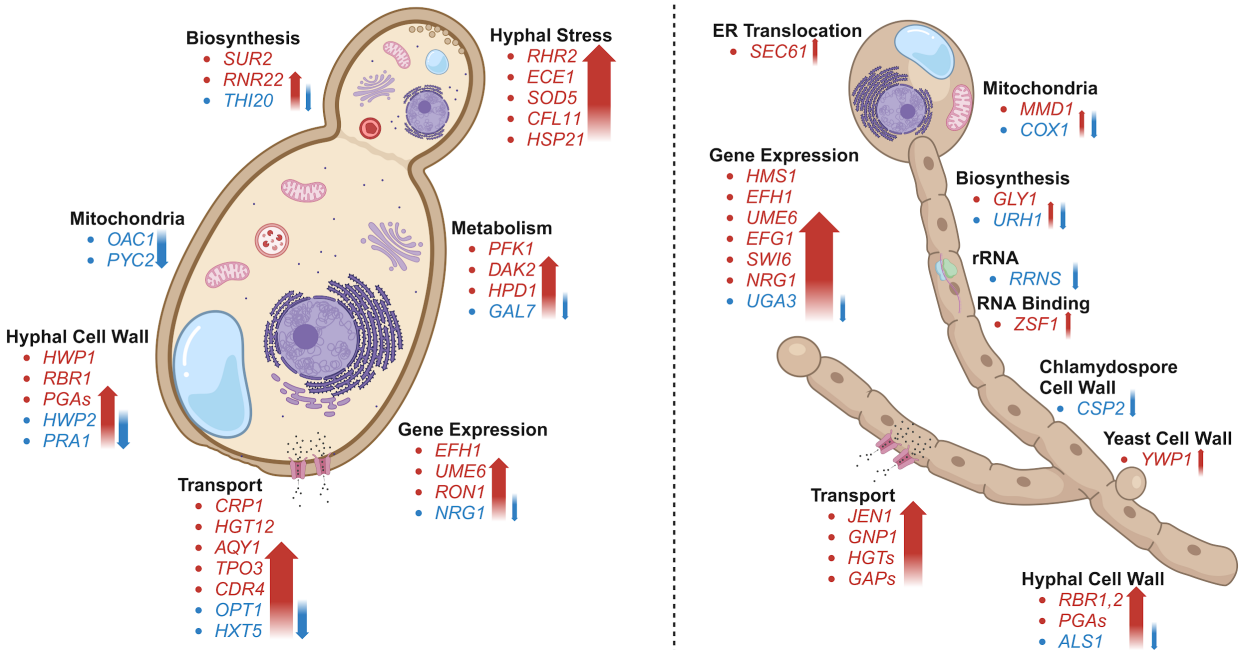

323

324 **Fig 8. Diagram of the *dhh1Δ/Δ* transcriptome in YPD and RPMI.** Under yeast-from growth
325 conditions *dhh1Δ/Δ* fails to repress the hyphal stress response. Under hyphal growth conditions
326 *dhh1Δ/Δ* presents a misregulated transcriptome. Genes in red were significantly upregulated in
327 *dhh1Δ/Δ*, while genes in blue were significantly downregulated in *dhh1Δ/Δ*.

328 Discussion

329 Foundational research on the genetic bases of filamentation largely focused on transcription
330 factors [9] such as *BRG1* [68], *UME6* [69], and *EFG1* [12]. More recently, growing evidence for
331 post-transcriptional regulation of filamentation has added an additional layer of control
332 [14,15,21]. Previous studies reported that loss of a single *DHH1* copy impairs filamentation [34]
333 and the requirement of *EDC3* for WT stress tolerance and filamentation [35,36]. These results
334 suggested PB factors have different functions in *C. albicans* as compared to their homologs in
335 *S. cerevisiae* and *S. pombe* [34,42,54,70,71]. However, the molecular methods originally used
336 to generate *C. albicans DHH1/dhh1Δ* and *edc3Δ/Δ* can lead to confounding effects that require
337 complementation assay controls [72–74]. Unlike *S. cerevisiae* [45,47,75], the gene regulatory
338 effects of *DHH1* deletion, both during yeast and hyphal growth, were not previously
339 characterized in *C. albicans*. Here we investigated the roles of PB factors Dhh1 and Edc3 in *C.*
340 *albicans* growth, filamentation, and gene expression.

341 Previous research reported Edc3 was necessary for observable PBs during *C. albicans* glucose
342 starvation [35]. Contrary to this, *S. cerevisiae* PBs continue to condense in the absence of many
343 individual protein factors, including Dhh1 and Edc3 [43]. Our findings align with the roles of
344 these genes in *S. cerevisiae* and other eukaryotes. In *C. albicans*, PBs condense during heat
345 shock without Dhh1 or Edc3 (Fig 1. D, E). Additionally, we found Dhh1 was both present in PBs
346 and cytoplasmically diffuse, suggesting a PB-independent RNA decay function in the cytoplasm
347 (Fig 1. B), like *S. cerevisiae* [43,44]. Our results suggest that, as in *S. cerevisiae* [26,43,76], the

348 absence of multiple scaffolding proteins would be required to completely disassemble *C.*
349 *albicans* P-bodies [26,43,76]. Thus, *C. albicans* PBs may share many of the well documented
350 functions and characteristics of their homologous condensates from *S. cerevisiae*.

351 Our phenotypic results differ from previous studies, in which haploinsufficiency in filamentation
352 was previously reported for *DHH1* [34] (Figs. 4-5). In the initial survey of our mutants,
353 DHH1/*dhh1Δ* did not present the growth or heat sensitivity defects found in our *dhh1Δ/Δ* strain
354 (Fig. 2 A & B). Additionally, we found that a single copy of *DHH1* in our complement strain was
355 sufficient for recovery of WT planktonic, biofilm, and colony filamentation (Figs. 4-5). It's
356 possible that only a single copy of *DHH1* is necessary for WT growth and filamentation because
357 it is not the rate limiting factor for mRNA decay. Additionally, we found that e *EDC3* is not
358 required for heat tolerance at 37°C or filamentation, contrary to prior work [35,36] (Fig. S1). Our
359 data show *C. albicans* Edc3 functions as a non-essential enhancer of mRNA decapping, as in
360 *S. cerevisiae* [52]. While *EDC3* may not be essential for filamentation, retaining this gene likely
361 confers an as of yet unknown evolutionary advantage to *C. albicans*. Although we found
362 different phenotypes for deletion of *DHH1* and *EDC3* than in prior studies, this earlier work used
363 a deletion approach that can cause off-target effects [72–74] and complementation studies to
364 confirm the deletions were not performed [34,35,77]. Our results highlight the power of targeted
365 deletion through CRISPR-Cas9 and the importance of complementation analysis of genetic
366 phenotypes.

367 Though not the focus of this study, we note that we have recapitulated the previously reported
368 filamentation defect found with deletion of the RNA decay factor *NOT5* [29–31] (Fig. S2). Our
369 *not5Δ/Δ* strain had a distinct phenotype from our *dhh1Δ/Δ* strain. Unlike *dhh1Δ/Δ*, *not5Δ/Δ* did
370 not have any growth defects or heat sensitivity on YPD plates (Fig S2. A-B). Interestingly, while
371 *dhh1Δ/Δ* formed wrinkled colonies indicative of hyphal growth on spider media (Fig 5. E),
372 *not5Δ/Δ* was completely filamentation repressed (Fig S2. C). These results suggest that specific

373 mRNA decay factors are required for distinct aspects of filamentation and stress responses. As
374 the transcriptomic consequences of *NOT5* deletion in *C. albicans* remain unknown, future work
375 is needed to investigate this aspect of *not5Δ/Δ* and other mRNA decay factors that produce
376 aberrant hyphal phenotypes.

377 Interestingly, *dhh1Δ/Δ* early germ tubes were less developed when measured by the length to
378 width ratio despite the overall larger cells (Fig. 4) and colonies on spider plates failed to invade
379 agar around colony margins, yet presented other aspects of hyphal morphology (Fig 5. E). In
380 seeming contradiction, *dhh1Δ/Δ* generated deeper biofilms (Fig 5. A-B) with a distinctly altered
381 structure, potentially due to the greater cell size and/or a slower cell cycle (Fig 5. C-D). These
382 apparently diametrical results are not uncommon in other *C. albicans* genetic backgrounds
383 where the same strain may have varied filamentation phenotypes under different conditions
384 [78]. Performing RNA-seq on *dhh1Δ/Δ* exposed to different filamentation conditions *in vitro* may
385 provide mechanistic evidence for our mixed hyphal phenotypes. In conclusion, the dysregulated
386 *dhh1Δ/Δ* transcriptome impacts cell, biofilm, and colony morphology but in a manner that is not
387 canonically filamentation impaired or hyperfilamentous.

388 Strikingly, we found the absence of *DHH1* induces major transcriptomic changes in both yeast
389 (YPD) and hyphae (RPMI) (Fig. 6). These changes suggest an “identity crisis”, such that the
390 deletion strain expresses hyphal genes under yeast-growth conditions (Fig. 8). Yeast-form
391 *dhh1Δ/Δ* upregulates genes normally associated with hyphal virulence such as *RHR2* [79],
392 *ECE1* [5], and *HWP1* [80] in YPD (Fig 6. A; Fig. S4-5). Additionally, upregulated genes are
393 enriched in cell wall and cell surface GO terms in yeast and hyphae (Fig 6. B, D). However,
394 *dhh1Δ/Δ* hyphae exhibit transcripts associated with a phenotypically hybrid cell wall. For
395 example, *dhh1Δ/Δ* hyphae upregulate the transcript for yeast cell wall protein *YWP1* and
396 downregulate adhesion transcript *ALS1* (Fig 6. C; Fig. S6). One interesting possibility is that the
397 absence of *DHH1* leads to environmentally inappropriate expression of vital transcription factors

398 regulating morphology (Fig 6. F). Upregulation of stress-associated genes in *C. albicans*
399 *dhh1Δ/Δ* YPD (cell wall and adhesion) and RPMI (cell wall, alternative carbohydrate/nitrogen
400 sources) are consistent with findings in *S. cerevisiae dhh1Δ/Δ* (Fig 6. B, D, Fig. 8) [47].
401 Comparing *dhh1Δ/Δ* RPMI to YPD, we find blunted transcriptome remodeling during
402 filamentation in contrast to WT (Fig 7. A, D). This is most likely due to upregulation of stress-
403 response genes in YPD and defective mRNA decay in the absence of *DHH1*.

404 The widespread, transcriptomic alterations in *C. albicans dhh1Δ/Δ* are likely responsible for the
405 large number of abnormal growth phenotypes. In YPD, upregulated transcription factors that are
406 positive regulators of hyphal growth include *EFH1*, *UME6*, and *RON1* [9] (Fig 6. F). Additionally,
407 hyphal repressor *NRG1* [57,58] was downregulated, potentially de-repressing downstream
408 hyphal associated genes in YPD (Fig 6. F). This TF profile could directly upregulate hyphal cell
409 wall genes associated with the wrinkled phenotypes [9,63,69] seen on YPD plates at 30°C and
410 37°C (Fig 2. A-C). Interestingly, under filamentation conditions *dhh1Δ/Δ* RPMI upregulated
411 select hyphal transcription factors to a greater extent than WT (*HMS1*, *UME6*, *EFH1*, and
412 *EFG1*) (Fig 6. F). In addition, the upregulation of *NRG1* in *dhh1Δ/Δ* under filamentous growth
413 conditions, may attenuate hyphal growth (Fig 6. F). Conversely, the hyphal TF *UGA3* was
414 significantly downregulated in filamentous *dhh1Δ/Δ* (Fig 6. F). This may be a subtle contributor
415 to abnormal filamentous growth, since the loss of *UGA3* is not associated with a phenotype *in*
416 *vitro*, but has reduced colonization *in vivo* [81]. The mixed TF profile in *dhh1Δ/Δ* RPMI induces a
417 complex hyphal phenotype that is both hypofilamentous in some assays, while being apparently
418 hyperfilamentous in a biofilm context. The blunted shift of TF expression in *dhh1Δ/Δ*
419 filamentation may be attributable to a premature hyphal transcriptome in *dhh1Δ/Δ* yeast (Fig 7.
420 G). In summary, the loss of *DHH1* not only impacts the direct targets of mRNA decay, but
421 downstream regulation of the yeast-to-hyphae gene regulatory network inducing transcriptomic
422 dysregulation and aberrant phenotypes.

423 In many species stochastic transcriptional noise serves as a form of “bet-hedging” for acute
424 environmental stressors [37–39]. For example, within a population of *C. albicans* individual cells
425 express Efg1 heterogeneously, adapting colonization to host immune status [82]. Our data
426 support a model where *C. albicans* adapts to diverse host microenvironments by transcribing
427 multiple stress-associated genes, while simultaneously buffering expression via mRNA decay.
428 This strategy promotes rapid responses to diverse stressors without investing energy towards
429 environmentally inappropriate proteomic and phenotypic remodeling. However, the role of Dhh1
430 and other mRNA decay factors in controlling expression of transcriptionally noisy genes
431 remains minimally investigated in *C. albicans*. There are two reported models in *S. cerevisiae*
432 for Dhh1 dependent mRNA decay, 1) slow translation and poor codon optimality [45,46] and 2)
433 repression of genes associated with nutrient limitation [47]. Contrary to the first model, genes
434 upregulated in *C. albicans dhh1Δ/Δ* had higher CAI values than genes downregulated in the
435 mutant, suggesting rare codons do not mark genes for Dhh1-mediated mRNA decay in *C.*
436 *albicans* (Fig. S7). However, we found that *C. albicans dhh1Δ/Δ* upregulates homologs relating
437 to cell wall and non-preferred carbon and nitrogen sources that were de-repressed in *S.*
438 *cerevisiae dhh1Δ* [47], correlating with the second model. Future work is needed to elucidate
439 the features of transcripts repressed by Dhh1 in *C. albicans* under different growth conditions.
440 For example, 4-thioU pulse-chase experiments could identify changes in RNA stability in the
441 *dhh1Δ/Δ* mutant to further investigate if Dhh1 promotes decay of noisy stress-response
442 transcripts. Future work using ribosome profiling could also help identify any role for Dhh1 in
443 translation during filamentation. Regardless of the outcomes of such studies, our work clearly
444 defines an important role for Dhh1 in regulating filamentous growth and gene expression in *C.*
445 *albicans*.

446 # Materials and methods

447 ## Strains and media

448 All strains used in this study are listed in Table S5. They were maintained as 15%
449 glycerol stocks stored at -80°C. Before all experiments, strains were grown on YPD (2%
450 Bacto Peptone, 2% dextrose, 1% yeast extract) agar plates for two days at 30°C. For acute heat
451 shock experiments, cells were grown in complete media (CM) (0.68% yeast nitrogenous base,
452 0.079% CSM complete AA mixture, 2% dextrose). The growth media for planktonic
453 filamentation and biofilm assays was RPMI 1640 (Gibco, - phenol red) supplemented with 10%
454 fetal bovine serum. We evaluated filamentous colony morphology with spider plates [83] (1%
455 nutrient broth, 1% D-mannitol, 0.2% K_2HPO_4, 2% agar).
456

457 ## Strain construction

458 WT SC5314 and transformation plasmids pV1093 and pRS316 were generously provided by
459 the Mitchell lab. All C-terminal fluorescent tags (Edc3-mNG and Dhh1-mS) were generated with
460 the SAT1 FLP/FRT transformation cassette [84] from the plasmid pRS316 [SAT1 flipper from
461 pSFS2] with *C. albicans* optimized mNeonGreen and mScarlet [85]. The SAT1 FLP/FRT
462 transformation cassette ligated to the gene for fluorescent protein was inserted into the C-
463 terminal end of the chromosomal gene using lithium acetate transformation. A subsequent
464 incubation in maltose containing media induced SAT1 excision leaving the C-terminal
465 fluorescent tag fused to the protein of interest. To generate the Dhh1-mS strains we
466 incorporated the transient CRISPR-cas9 system for improved transformation efficiency [55].
467 Optimal cas9 PAM sites were selected from a database of sites [86].
468

469 *DHH1* deletion (*DHH1/dhh1Δ*, *dhh1Δ/Δ*), complement (*dhh1Δ/Δ, +DHH1; dhh1Δ/Δ,*
470 *+DHH1/DHH1*), and overexpression strains (WT, *+DHH1*; WT, *+DHH1/DHH1*) were generated
471 in SC5314 with the SAT1 FLP/FRT and transient CRISPR-cas9 approach [55,84]. To insert a

472 copy of DHH1 into the SC5314 genome for complement and overexpression strains we inserted
473 *DHH1* fused to the *TPI1* promoter at the *MDR1* site. The SC5314 homozygous *EDC3* and
474 *NOT5* deletion strains (*edc3Δ/Δ, not5Δ/Δ*) were generated using the same SAT1 FLP/FRT and
475 transient CRISPR-cas9 approach.
476
477 All strains generated for this paper were validated by gDNA PCR for cassette insertion,
478 homo/heterozygosity, and excision of SAT1. We used *TDH3* as the control for gDNA extraction
479 and amplification. All strains, plasmids, and primers for strain construction and verification are
480 listed in Table S5.
481

482 Phenotype assays

483 For spot plates, strains were grown overnight at 30°C in liquid YPD, diluted to an OD_{600} of 0.5
484 and serially diluted 10-fold. YPD plates were spotted with 5µL of diluted cells and incubated for
485 1-3 days at 30°C and 37°C.

486 To evaluate planktonic filamentation we grew strains overnight at 30°C in liquid YPD, diluted
487 them to an OD_{600} of 0.2 and subcultured them to an OD_{600} of 0.6 before washing and inducing
488 physiologically relevant filamentation conditions (RPMI + 10% serum, 37°C). After a
489 filamentation period of 4 or 16 hours cells were fixed with 4% formalin, washed with PBS, and
490 stained with calcofluor white.

491 To survey biofilm growth, we grew cells overnight at 30°C in YPD and diluted them to an OD_{600}
492 of 0.33 in RPMI + 10% serum. Four replicates of diluted cells were added to a 96-well ibidi plate
493 coated with polyallylamine (PA) and incubated for 90-minutes at 37ºC for adherence. After 90
494 minutes, the media was replaced leaving only adherent cells. After a 24-hour incubation at

495 37°C, cells were fixed with 4% formalin, washed with PBS, and stained with ConA Alexa Fluor
496 594 conjugate prior to confocal imaging.

497 For the 6-day spider plate colony assay, strains were grown overnight at 30°C in liquid YPD,
498 harvested by centrifugation and washed with PBS. The washed cells were diluted to an OD_{600} of
499 0.33 in PBS and 3μL was spotted onto spider plates. Plates were incubated for 6 days at 37°C
500 with humidity. The same method was used for the 37°C 4-day YPD plate colony assay.

501 To evaluate exponential growth and cellular morphology in liquid YPD, strains were grown
502 overnight at 30°C in YPD. The next morning cells were diluted to an OD_{600} of 0.05 and
503 incubated at 30°C for 14 hours. The OD_{600} was recorded hourly and live cells were imaged at 5
504 hours.

505 Imaging

506 Single-cell fluorescent, DIC, and transmitted light images were captured with a Zeiss Axiovert
507 200 using a 100X Plan-NEOFLUAR, 25X Plan-Apochromat, and 40X Plan-Apochromat
508 objectives. Confocal images were captured with a 50-micron confocal slit wheel. Spot plates
509 were documented using a BIO-RAD ChemiDoc Touch Imaging System. Images of colonies 4
510 and 6-day colonies on YPD and spider media. were collected with a Wild M8 Heerbrugg Stereo
511 Microscope.
512

513 RNA-extraction and sequencing

514 All experimental strains and conditions were completed in triplicate (WT YPD, WT RPMI,
515 *dhh1Δ/Δ* YPD, *dhh1Δ/Δ* RPMI for a total of 12 samples. SC5314 WT and *dhh1Δ/Δ* strains were
516 grown overnight at 30°C in liquid YPD and diluted to an OD_{600} of 0.2 in liquid YPD the next
517 morning. Sub-cultured cells were grown in YPD at 30°C until the OD_{600} reached 0.8. Yeast cells
518 were collected by centrifugation and frozen in liquid nitrogen. The remaining yeast cells were

519 washed and grown under physiologically relevant filamentation conditions (RPMI + 10% serum
520 at 37°C) for 4 hours. The early filamenting hyphae were collected by 0.2μm sterile filtration and
521 frozen in liquid nitrogen. Cell pellets were stored at -80°C prior to RNA extraction.

522 Frozen cells were resuspended in cold RNA buffer (4M NaCl, 1MTris-HCl pH7.5, EDTA) and
523 vortexed with zirconia beads. To extract RNA from the resuspended cells we added acid phenol
524 and continued 10 cycles of vortexing and chilling. After centrifugation, the aqueous phase was
525 removed and transferred to a clean tube with an equal volume of chloroform. After a second
526 centrifugation the aqueous phase was removed again and added to 3X volume of ice cold 100%
527 ethanol. To precipitate the RNA, the tube was incubated in a -80°C for a minimum of 30
528 minutes. After centrifugation the RNA pellet was washed with 70% ice cold ethanol and the RNA
529 pellet was resuspended in ultrapure water. Genomic DNA was removed using a ThermoFisher
530 TURBO DNA-free kit, and we re-extracted the RNA with Trizol and chloroform. The RNA was
531 cleaned and concentrated using a kit from Zymo. RNA quantity was measured by nanodrop and
532 the RIN^{e} was quantified using an Aglient TapeStation. Strand-specific,150bp-paired ends were
533 sequenced by Novogene.

534

535 Transcript alignment, quantification, and quality control

536 Reads were aligned to the *C. albicans* release 22 using HISAT2 [87]. SAMTools [88] was used
537 to generate primary hits and bigWig coverage tracks for IGV [89]. Coverage tracks of select
538 genes are shown in Fig S3-6. We confirmed that *DHH1* transcripts were present in WT cells and
539 absent in *dhh1Δ/Δ* under both growth conditions (Fig S3). We quantified the number of
540 transcripts in each strain (WT, *dhh1Δ/Δ*) and growth condition (YPD, RPMI) with BEDTools [90].
541 All 12 experimental groups were combined into a single file of raw hits using a custom perl [91]
542 script). Using edgeR [92] we converted raw hits to unfiltered copies to million (Fig S8. A). Poorly

543 transcribed ORFs (<1 CPM in <3 groups) were screened out leaving only hits with ≥1 CPM in

544 ≥3 groups (Fig S8. B). Using the built-in R function prcomp we performed a principal component

545 analysis to identify factors that separate samples. Our experimental replicates are clustered by

546 strain and growth conditions (Fig S9).

547 Software and data analysis

548 All images were processed with Fiji [93]. Length to width ratios of 4 and 16-hour filamenting

549 planktonic cells and biofilm depth were quantified in Fiji using the ROI manager. Primers and

550 transformation cassettes were designed using sequences from the *Candida* Genome Database

551 [94] and the *Candida albicans* Umbrella Comparative genomics project [95], NCBI bioproject ID:

552 PRJNA193498. Codon adaptation index (CAI) was calculated using CAIcal [96] and codon

553 usage table from the *Candida* Genome database [94]. Data analysis and statistical tests were

554 performed using GraphPad Prism version 10.0.0 for Windows [97] as well as R [98] with ggplot2

555 [99] and DESeq2 [100] packages. We used Affinity Designer for Windows Version 1.10.6, 2020

556 and BioRender.com to compose our figures.

557 Acknowledgements

558 We would like to thank Gemma E. May for her cloning expertise and support as well as the

559 members of the McManus laboratory for helpful discussions.

560 References

561 1. Brown GD, Denning DW, Gow NAR, Levitz SM, Netea MG, White TC. Hidden killers:
562 human fungal infections. Sci Transl Med. 2012 Dec 19;4(165):165rv13.

563 2. Kullberg BJ, Arendrup MC. Invasive Candidiasis. N Engl J Med. 2015 Oct 8;373(15):1445–
564 56.

565 3. Kadosh D, Lopez-Ribot JL. Candida albicans: adapting to succeed. Cell Host Microbe.

566 2013 Nov 13;14(5):483–5.

567 4. Brown AJP, Budge S, Kaloriti D, Tillmann A, Jacobsen MD, Yin Z, et al. Stress adaptation
568 in a pathogenic fungus. J Exp Biol. 2014 Jan 1;217(Pt 1):144–55.

569 5. Moyes DL, Wilson D, Richardson JP, Mogavero S, Tang SX, Wernecke J, et al.
570 Candidalysin is a fungal peptide toxin critical for mucosal infection. Nature. 2016 Apr
571 7;532(7597):64–8.

572 6. Desai JV, Mitchell AP. Candida albicans Biofilm Development and Its Genetic Control.
573 Microbiol Spectr [Internet]. 2015 Jun;3(3). Available from:
574 http://dx.doi.org/10.1128/microbiolspec.MB-0005-2014

575 7. Finkel JS, Mitchell AP. Genetic control of Candida albicans biofilm development. Nat Rev
576 Microbiol. 2011 Feb;9(2):109–18.

577 8. Chandra Jyotsna, Kuhn Duncan M., Mukherjee Pranab K., Hoyer Lois L., McCormick
578 Thomas, Ghannoum Mahmoud A. Biofilm Formation by the Fungal Pathogen Candida
579 albicans: Development, Architecture, and Drug Resistance. J Bacteriol. 2001 Sep
580 15;183(18):5385–94.

581 9. Villa S, Hamideh M, Weinstock A, Qasim MN, Hazbun TR, Sellam A, et al. Transcriptional
582 control of hyphal morphogenesis in Candida albicans. FEMS Yeast Res [Internet]. 2020
583 Feb 1;20(1). Available from: http://dx.doi.org/10.1093/femsyr/foaa005

584 10. Chen H, Zhou X, Ren B, Cheng L. The regulation of hyphae growth in Candida albicans.
585 Virulence. 2020 Dec;11(1):337–48.

586 11. Martin R, Albrecht-Eckardt D, Brunke S, Hube B, Hünniger K, Kurzai O. A core
587 filamentation response network in Candida albicans is restricted to eight genes. PLoS One.
588 2013 Mar 14;8(3):e58613.

589 12. Glazier VE. EFG1, Everyone's Favorite Gene in Candida albicans: A Comprehensive
590 Literature Review. Front Cell Infect Microbiol. 2022 Mar 22;12:855229.

591 13. Azadmanesh J, Gowen AM, Creger PE, Schafer ND, Blankenship JR. Filamentation
592 Involves Two Overlapping, but Distinct, Programs of Filamentation in the Pathogenic
593 Fungus Candida albicans. G3 . 2017 Nov 6;7(11):3797–808.

594 14. Kadosh D. Control of Candida albicans morphology and pathogenicity by post-
595 transcriptional mechanisms. Cell Mol Life Sci. 2016 Nov;73(22):4265–78.

596 15. Verma-Gaur J, Traven A. Post-transcriptional gene regulation in the biology and virulence
597 of Candida albicans. Cell Microbiol. 2016 Jun;18(6):800–6.

598 16. Pizzinga M, Harvey RF, Garland GD, Mordue R, Dezi V, Ramakrishna M, et al. The cell
599 stress response: extreme times call for post-transcriptional measures. Wiley Interdiscip Rev
600 RNA. 2020 May;11(3):e1578.

601 17. Hernández-Elvira M, Sunnerhagen P. Post-transcriptional regulation during stress. FEMS
602 Yeast Res [Internet]. 2022 Jun 30;22(1). Available from:
603 http://dx.doi.org/10.1093/femsyr/foac025

604 18. Keene JD. RNA regulons: coordination of post-transcriptional events. Nat Rev Genet. 2007
605 Jul;8(7):533–43.

606 19. Halbeisen RE, Galgano A, Scherrer T, Gerber AP. Post-transcriptional gene regulation:
607 from genome-wide studies to principles. Cell Mol Life Sci. 2008 Mar;65(5):798–813.

608 20. Bloom ALM, Leipheimer J, Panepinto JC. mRNA decay: an adaptation tool for the
609 environmental fungal pathogen Cryptococcus neoformans. Wiley Interdiscip Rev RNA
610 [Internet]. 2017 Sep;8(5). Available from: http://dx.doi.org/10.1002/wrna.1424

611 21. Rana A, Gupta N, Thakur A. Post-transcriptional and translational control of the morphology
612 and virulence in human fungal pathogens. Mol Aspects Med. 2021 Oct;81:101017.

613 22. Balagopal V, Parker R. Polysomes, P bodies and stress granules: states and fates of
614 eukaryotic mRNAs. Curr Opin Cell Biol. 2009 Jun;21(3):403–8.

615 23. Youn JY, Dyakov BJA, Zhang J, Knight JDR, Vernon RM, Forman-Kay JD, et al. Properties
616 of Stress Granule and P-Body Proteomes. Mol Cell. 2019 Oct 17;76(2):286–94.

617 24. Mugler CF, Hondele M, Heinrich S, Sachdev R, Vallotton P, Koek AY, et al. ATPase activity
618 of the DEAD-box protein Dhh1 controls processing body formation. Elife [Internet]. 2016
619 Oct 3;5. Available from: http://dx.doi.org/10.7554/eLife.18746

620 25. Collart MA. The Ccr4-Not complex is a key regulator of eukaryotic gene expression. Wiley
621 Interdiscip Rev RNA. 2016 Jul;7(4):438–54.

622 26. Teixeira D, Sheth U, Valencia-Sanchez MA, Brengues M, Parker R. Processing bodies
623 require RNA for assembly and contain nontranslating mRNAs. RNA. 2005 Apr;11(4):371–
624 82.

625 27. Protter DSW, Parker R. Principles and Properties of Stress Granules. Trends Cell Biol.
626 2016 Sep;26(9):668–79.

627 28. Dagley MJ, Gentle IE, Beilharz TH, Pettolino FA, Djordjevic JT, Lo TL, et al. Cell wall
628 integrity is linked to mitochondria and phospholipid homeostasis in Candida albicans
629 through the activity of the post-transcriptional regulator Ccr4-Pop2. Mol Microbiol. 2011
630 Feb;79(4):968–89.

631 29. Cheng S, Clancy CJ, Checkley MA, Handfield M, Hillman JD, Progulske-Fox A, et al.
632 Identification of Candida albicans genes induced during thrush offers insight into
633 pathogenesis. Mol Microbiol. 2003 Jun;48(5):1275–88.

634 30. Cheng S, Nguyen MH, Zhang Z, Jia H, Handfield M, Clancy CJ. Evaluation of the roles of
635 four Candida albicans genes in virulence by using gene disruption strains that express
636 URA3 from the native locus. Infect Immun. 2003 Oct;71(10):6101–3.

637 31. Cheng S, Clancy CJ, Checkley MA, Zhang Z, Wozniak KL, Seshan KR, et al. The role of
638 Candida albicans NOT5 in virulence depends upon diverse host factors in vivo. Infect
639 Immun. 2005 Nov;73(11):7190–7.

640 32. Richard ML, Nobile CJ, Bruno VM, Mitchell AP. Candida albicans biofilm-defective mutants.
641 Eukaryot Cell. 2005 Aug;4(8):1493–502.

642 33. An HS, Lee KH, Kim J. Identification of an exoribonuclease homolog, CaKEM1/CaXRN1, in
643 Candida albicans and its characterization in filamentous growth. FEMS Microbiol Lett. 2004
644 Jun 1;235(2):297–303.

645 34. Shively CA, Kweon HK, Norman KL, Mellacheruvu D, Xu T, Sheidy DT, et al. Large-Scale
646 Analysis of Kinase Signaling in Yeast Pseudohyphal Development Identifies Regulation of
647 Ribonucleoprotein Granules. PLoS Genet. 2015 Oct;11(10):e1005564.

648 35. Jung JH, Kim J. Accumulation of P-bodies in Candida albicans under different stress and
649 filamentous growth conditions. Fungal Genet Biol. 2011 Dec;48(12):1116–23.

650 36. Jung JH, Kim J. Roles of Edc3 in the oxidative stress response and CaMCA1-encoded
651 metacaspase expression in Candida albicans. FEBS J. 2014 Nov;281(21):4841–51.

652 37. Raser JM, O'Shea EK. Noise in gene expression: origins, consequences, and control.
653 Science. 2005 Sep 23;309(5743):2010–3.

654 38. Zhuravel D, Fraser D, St-Pierre S, Tepliakova L, Pang WL, Hasty J, et al. Phenotypic
655 impact of regulatory noise in cellular stress-response pathways. Syst Synth Biol. 2010
656 Jun;4(2):105–16.

657 39. Urban EA, Johnston RJ Jr. Buffering and Amplifying Transcriptional Noise During Cell Fate
658 Specification. Front Genet. 2018 Nov 29;9:591.

659 40. Timmers HTM, Tora L. Transcript Buffering: A Balancing Act between mRNA Synthesis and
660 mRNA Degradation. Mol Cell. 2018 Oct 4;72(1):10–7.

661 41. Palenchar PM, DeStefanis T. Transcriptional noise adjusted for expression levels reveals
662 genes with high transcriptional noise that are highly expressed, functionally related, and co-
663 regulated in yeast. Curr Genet. 2022 Dec;68(5-6):675–86.

664 42. Nissan T, Rajyaguru P, She M, Song H, Parker R. Decapping activators in Saccharomyces
665 cerevisiae act by multiple mechanisms. Mol Cell. 2010 Sep 10;39(5):773–83.

666 43. Rao BS, Parker R. Numerous interactions act redundantly to assemble a tunable size of P
667 bodies in Saccharomyces cerevisiae. Proc Natl Acad Sci U S A. 2017 Nov
668 7;114(45):E9569–78.

669 44. Carroll JS, Munchel SE, Weis K. The DExD/H box ATPase Dhh1 functions in translational
670 repression, mRNA decay, and processing body dynamics. J Cell Biol. 2011 Aug
671 22;194(4):527–37.

672 45. Sweet T, Kovalak C, Coller J. The DEAD-box protein Dhh1 promotes decapping by slowing
673 ribosome movement. PLoS Biol. 2012 Jun 12;10(6):e1001342.

674 46. Radhakrishnan A, Chen YH, Martin S, Alhusaini N, Green R, Coller J. The DEAD-Box
675 Protein Dhh1p Couples mRNA Decay and Translation by Monitoring Codon Optimality.
676 Cell. 2016 Sep 22;167(1):122–32.e9.

677 47. Vijjamarri AK, Gupta N, Onu C, Niu X, Zhang F, Kumar R, et al. mRNA decapping
678 activators Pat1 and Dhh1 regulate transcript abundance and translation to tune cellular
679 responses to nutrient availability. Nucleic Acids Res. 2023 Sep 22;51(17):9314–36.

680 48. Jungfleisch J, Nedialkova DD, Dotu I, Sloan KE, Martinez-Bosch N, Brüning L, et al. A
681 novel translational control mechanism involving RNA structures within coding sequences.
682 Genome Res. 2017 Jan;27(1):95–106.

683 49. Park YU, Hur H, Ka M, Kim J. Identification of translational regulation target genes during
684 filamentous growth in Saccharomyces cerevisiae: regulatory role of Caf20 and Dhh1.
685 Eukaryot Cell. 2006 Dec;5(12):2120–7.

686 50. Ka M, Park YU, Kim J. The DEAD-box RNA helicase, Dhh1, functions in mating by
687 regulating Ste12 translation in Saccharomyces cerevisiae. Biochem Biophys Res Commun.
688 2008 Mar 14;367(3):680–6.

689 51. Lee E, Jung D, Kim J. Roles of Dhh1 RNA helicase in yeast filamentous growth: Analysis of
690 N-terminal phosphorylation residues and ATPase domains. J Microbiol. 2020
691 Oct;58(10):853–8.

692 52. Kshirsagar M, Parker R. Identification of Edc3p as an enhancer of mRNA decapping in
693 Saccharomyces cerevisiae. Genetics. 2004 Feb;166(2):729–39.

694 53. Decker CJ, Teixeira D, Parker R. Edc3p and a glutamine/asparagine-rich domain of Lsm4p
695 function in processing body assembly in Saccharomyces cerevisiae. J Cell Biol. 2007 Nov
696 5;179(3):437–49.

697 54. Wang CY, Chen WL, Wang SW. Pdc1 functions in the assembly of P bodies in
698 Schizosaccharomyces pombe. Mol Cell Biol. 2013 Mar;33(6):1244–53.

699 55. Huang MY, Cravener MC, Mitchell AP. Targeted Genetic Changes in Candida albicans
700 Using Transient CRISPR-Cas9 Expression. Curr Protoc. 2021 Jan;1(1):e19.

701 56. Xing W, Muhlrad D, Parker R, Rosen MK. A quantitative inventory of yeast P body proteins
702 reveals principles of composition and specificity. Elife [Internet]. 2020 Jun 19;9. Available
703 from: http://dx.doi.org/10.7554/eLife.56525

704 57. Murad A, Leng P, Straffon M, Wishart J, Macaskill S, MacCallum D, et al. NRG1 represses
705 yeast–hypha morphogenesis and hypha-specific gene expression in Candida albicans.
706 EMBO J [Internet]. 2001 Sep 3;20. Available from:
707 http://emboj.embopress.org/cgi/doi/10.1093/emboj/20.17.4742

708 58. Braun BR, Kadosh D, Johnson AD. NRG1, a repressor of filamentous growth in C.albicans,
709 is down-regulated during filament induction. EMBO J. 2001;20(17).

710 59. LaFayette SL, Collins C, Zaas AK, Schell WA, Betancourt-Quiroz M, Gunatilaka AAL, et al.
711 PKC signaling regulates drug resistance of the fungal pathogen Candida albicans via
712 circuitry comprised of Mkc1, calcineurin, and Hsp90. PLoS Pathog. 2010 Aug
713 26;6(8):e1001069.

714 60. Xie JL, Qin L, Miao Z, Grys BT, Diaz JDLC, Ting K, et al. The Candida albicans
715 transcription factor Cas5 couples stress responses, drug resistance and cell cycle
716 regulation. Nat Commun. 2017 Sep 11;8(1):499.

717 61. Bruno VM, Wang Z, Marjani SL, Euskirchen GM, Martin J, Sherlock G, et al.
718 Comprehensive annotation of the transcriptome of the human fungal pathogen Candida

719 albicans using RNA-seq. Genome Res. 2010 Oct;20(10):1451–8.

720 62. Carlisle PL, Kadosh D. A genome-wide transcriptional analysis of morphology
721 determination in Candida albicans. Mol Biol Cell. 2013 Feb;24(3):246–60.

722 63. Kadosh D, Johnson AD. Induction of the Candida albicans Filamentous Growth Program by
723 Relief of Transcriptional Repression: A Genome-wide Analysis. carried out (Odds.
724 2004;1985:1988.

725 64. Wakade RS, Wellington M, Krysan DJ. Temporal dynamics of Candida albicans
726 morphogenesis and gene expression reveals distinctions between in vitro and in vivo
727 filamentation. mSphere. 2024 Mar 19;e0011024.

728 65. Nantel A, Dignard D, Bachewich C, Harcus D, Marcil A, Bouin AP, et al. Transcription
729 profiling of Candida albicans cells undergoing the yeast-to-hyphal transition. Mol Biol Cell.
730 2002 Oct;13(10):3452–65.

731 66. Nobile CJ, Fox EP, Nett JE, Sorrells TR, Mitrovich QM, Hernday AD, et al. A recently
732 evolved transcriptional network controls biofilm development in Candida albicans. Cell.
733 2012 Jan 20;148(1-2):126–38.

734 67. Enjalbert B, Nantel A, Whiteway M. Stress-induced gene expression in Candida albicans:
735 absence of a general stress response. Mol Biol Cell. 2003 Apr;14(4):1460–7.

736 68. Cleary IA, Lazzell AL, Monteagudo C, Thomas DP, Saville SP. BRG1 and NRG1 form a
737 novel feedback circuit regulating Candida albicans hypha formation and virulence. Mol
738 Microbiol. 2012 Aug;85(3):557–73.

739 69. Banerjee M, Thompson DS, Lazzell A, Carlisle PL, Pierce C, Monteagudo C, et al. UME6, a
740 novel filament-specific regulator of Candida albicans hyphal extension and virulence. Mol
741 Biol Cell. 2008 Apr;19(4):1354–65.

742 70. Dong S, Li C, Zenklusen D, Singer RH, Jacobson A, He F. YRA1 autoregulation requires
743 nuclear export and cytoplasmic Edc3p-mediated degradation of its pre-mRNA. Mol Cell.
744 2007 Feb 23;25(4):559–73.

745 71. He F, Li C, Roy B, Jacobson A. Yeast Edc3 targets RPS28B mRNA for decapping by
746 binding to a 3' untranslated region decay-inducing regulatory element. Mol Cell Biol. 2014
747 Apr;34(8):1438–51.

748 72. Wellington M, Rustchenko E. 5-Fluoro-orotic acid induces chromosome alterations in
749 Candida albicans. Yeast. 2005 Jan 15;22(1):57–70.

750 73. Lay J, Henry LK, Clifford J, Koltin Y, Bulawa CE, Becker JM. Altered expression of
751 selectable marker URA3 in gene-disrupted Candida albicans strains complicates
752 interpretation of virulence studies. Infect Immun. 1998 Nov;66(11):5301–6.

753 74. Brand Alexandra, MacCallum Donna M., Brown Alistair J. P., Gow Neil A. R., Odds Frank
754 C. Ectopic Expression of URA3 Can Influence the Virulence Phenotypes and Proteome of
755 Candida albicans but Can Be Overcome by Targeted Reintegration of URA3 at the RPS10
756 Locus. Eukaryot Cell. 2004 Aug 1;3(4):900–9.

757 75. Vijjamarri AK, Niu X, Vandermeulen MD, Onu C, Zhang F, Qiu H, et al. Decapping factor

758 Dcp2 controls mRNA abundance and translation to adjust metabolism and filamentation to
759 nutrient availability. Elife [Internet]. 2023 Jun 2;12. Available from:
760 http://dx.doi.org/10.7554/eLife.85545

761 76. Matheny T, Rao BS, Parker R. Transcriptome-Wide Comparison of Stress Granules and P-
762 Bodies Reveals that Translation Plays a Major Role in RNA Partitioning. Mol Cell Biol
763 [Internet]. 2019 Dec 15;39(24). Available from: http://dx.doi.org/10.1128/MCB.00313-19

764 77. Kim EC, Kim J. Deletion analysis of LSm, FDF, and YjeF domains of Candida albicans
765 Edc3 in hyphal growth and oxidative-stress response. J Microbiol. 2015 Feb;53(2):111–5.

766 78. Brandquist ND, Lampman C, Smith EJ, Basilio L, Almansob A, Iwen PC, et al. Significant
767 variation of filamentation phenotypes in clinical Candida albicans strains. Front Cell Infect
768 Microbiol [Internet]. 2023;13. Available from:
769 https://www.frontiersin.org/articles/10.3389/fcimb.2023.1207083

770 79. Desai JV, Cheng S, Ying T, Nguyen MH, Clancy CJ, Lanni F, et al. Coordination of Candida
771 albicans Invasion and Infection Functions by Phosphoglycerol Phosphatase Rhr2.
772 Pathogens. 2015 Jul 24;4(3):573–89.

773 80. Staab JF, Bradway SD, Fidel PL, Sundstrom P. Adhesive and mammalian
774 transglutaminase substrate properties of Candida albicans Hwp1. Science. 1999 Mar
775 5;283(5407):1535–8.

776 81. Vandeputte P, Ischer F, Sanglard D, Coste AT. In vivo systematic analysis of Candida
777 albicans Zn2-Cys6 transcription factors mutants for mice organ colonization. PLoS One.
778 2011 Oct 31;6(10):e26962.

779 82. Pierce JV, Kumamoto CA. Variation in Candida albicans EFG1 expression enables host-
780 dependent changes in colonizing fungal populations. MBio. 2012 Jul 24;3(4):e00117–12.

781 83. Cihlar RL, Calderone RA. Candida albicans: methods and protocols. Preface. Methods Mol
782 Biol. 2009;499:v.

783 84. Sasse C, Morschhäuser J. Gene deletion in Candida albicans wild-type strains using the
784 SAT1-flipping strategy. Methods Mol Biol. 2012;845:3–17.

785 85. Frazer C, Hernday AD, Bennett RJ. Monitoring Phenotypic Switching in Candida albicans
786 and the Use of Next-Gen Fluorescence Reporters. Curr Protoc Microbiol. 2019
787 Jun;53(1):e76.

788 86. Vyas VK, Barrasa MI, Fink GR. A Candida albicans CRISPR system permits genetic
789 engineering of essential genes and gene families. Sci Adv. 2015;1(3):e1500248.

790 87. Kim D, Paggi JM, Park C, Bennett C, Salzberg SL. Graph-based genome alignment and
791 genotyping with HISAT2 and HISAT-genotype. Nat Biotechnol. 2019 Aug;37(8):907–15.

792 88. Danecek P, Bonfield JK, Liddle J, Marshall J, Ohan V, Pollard MO, et al. Twelve years of
793 SAMtools and BCFtools. Gigascience [Internet]. 2021 Feb 16;10(2). Available from:
794 http://dx.doi.org/10.1093/gigascience/giab008

795 89. Robinson JT, Thorvaldsdóttir H, Winckler W, Guttman M, Lander ES, Getz G, et al.
796 Integrative genomics viewer. Nat Biotechnol. 2011 Jan;29(1):24–6.

797 90. Quinlan AR, Hall IM. BEDTools: a flexible suite of utilities for comparing genomic features.
798 Bioinformatics. 2010 Mar 15;26(6):841–2.

799 91. Wall L, Christiansen T, Orwant J. Programming perl. " O'Reilly Media, Inc."; 2000.

800 92. Robinson MD, McCarthy DJ, Smyth GK. edgeR: a Bioconductor package for differential
801 expression analysis of digital gene expression data. Bioinformatics. 2010 Jan 1;26(1):139–
802 40.

803 93. Schindelin J, Arganda-Carreras I, Frise E, Kaynig V, Longair M, Pietzsch T, et al. Fiji: an
804 open-source platform for biological-image analysis. Nat Methods. 2012 Jun 28;9(7):676–82.

805 94. Skrzypek MS, Binkley J, Sherlock G. Using the Candida Genome Database. Methods Mol
806 Biol. 2018;1757:31–47.

807 95. Hirakawa MP, Martinez DA, Sakthikumar S, Anderson MZ, Berlin A, Gujja S, et al. Genetic
808 and phenotypic intra-species variation in Candida albicans. Genome Res. 2015
809 Mar;25(3):413–25.

810 96. Puigbò P, Bravo IG, Garcia-Vallve S. CAIcal: a combined set of tools to assess codon
811 usage adaptation. Biol Direct. 2008 Sep 16;3:38.

812 97. Swift ML. GraphPad Prism, Data Analysis, and Scientific Graphing. J Chem Inf Comput Sci.
813 1997 Mar 1;37(2):411–2.

814 98. R Core Team. R: A Language and Environment for Statistical Computing [Internet]. Vienna,
815 Austria: R Foundation for Statistical Computing; 2021. Available from: https://www.R-
816 project.org/

817 99. Wickham H. ggplot2: Elegant Graphics for Data Analysis [Internet]. Springer-Verlag New
818 York; 2016. Available from: https://ggplot2.tidyverse.org

819 100. Love MI, Huber W, Anders S. Moderated estimation of fold change and dispersion for
820 RNA-seq data with DESeq2. Genome Biol. 2014;15(12):550.

821

822 # Supporting information

823 **Fig S1. Absence of *EDC3* does not impair growth or hyphal morphology.** WT and *edc3Δ/Δ*
824 were subjected to growth, filamentation, biofilm, and spider plate assays. **A.** 24-hour spot plate
825 assay of *C. albicans* WT and *edc3Δ/Δ*. **B.** WT and *edc3Δ/Δ* strains were subjected to a
826 planktonic 4-hour filamentation assay (37°C, RPMI + 10% serum). Scale bar = 20μm. **C.** Germ
827 tube development during planktonic filamentation was quantified by measuring the length by

828 width of 100 cells in at least 4 fields of view. (No significant difference between WT and *edc3Δ/Δ*
829 by Kruskal-Wallis test). **D.** Side-view of WT and *edc3Δ/Δ* strains after a 24-hour biofilm assay
830 (37°C, RPMI + 10% serum). Scale bar = 100μm. **E.** Replicate biofilm assays revealed
831 overlapping depth of WT and *edc3Δ/Δ* strains. Bars indicate averages and 95% confidence
832 intervals. **F.** Colonies from a spider plate assay (37°C) did not display a phenotypic defect in
833 *edc3Δ/Δ*. 6X and 25X magnification.

834 **Fig S2. Absence of *NOT5* grows like WT on YPD but fails to filament on spider media.** We
835 independently produced a *not5Δ/Δ* mutant in the SC5315 background. **A.** 30°C spot plate
836 assay of WT SC5314 and *not5Δ/Δ*. **B.** 37°C spot plate assay of WT SC5314 and *not5Δ/Δ*. **C.** 6-
837 day spider plate assay of SC5314 and *not5Δ/Δ*.

838 **Fig S3. *DHH1* transcripts are present in WT and absent from *dhh1Δ/Δ*.** Normalized IGV
839 tracks of *DHH1* transcripts from a representative of each experimental group.

840 **Fig S4. Hyphal associated glycerol 3-phosphatase (*RHR2*) transcripts are present in**
841 ***dhh1Δ/Δ* and absent in WT under yeast-form growth conditions.** Normalized IGV tracks of
842 *RHR2* in all 3 replicates of WT and *dhh1Δ/Δ* grown in YPD at 30°C.

843 **Fig S5. Hyphal associated candidalysin (*ECE1*) transcripts are upregulated in *dhh1Δ/Δ***
844 **compared to WT under yeast-form growth conditions.** Normalized IGV tracks of *ECE1* in all
845 3 replicates of WT and *dhh1Δ/Δ* grown in YPD at 30°C.

846 **Fig S6. Yeast associated yeast cell wall protein (*YWP1*) transcripts are present in**
847 ***dhh1Δ/Δ* and absent in WT under hyphae-inducing conditions.** Normalized IGV tracks of
848 *YWP1* in all 3 replicates of WT and *dhh1Δ/Δ* strains grown in RPMI + serum at 37°C for 4 hours.

849 **Fig S7. Upregulated genes in *C. albicans dhh1Δ/Δ* have higher CAI values than**
850 **downregulated genes.** CAIs of 100 most upregulated and downregulated genes in **A.** YPD and
851 **B.** RPMI. (Mann-Whitney test. ***P = 0.0008, ****P < 0.0001).

852 **Fig S8. Filtering out poorly transcribed ORFs in normalized RNAseq hits.** ORFs with less
853 than one CPM hit in less than 3 experimental groups were removed prior to running DEseq2. **A.**
854 Violin plots show raw and **B.** filtered hits for each experimental group with ≥1 CPM in ≥3
855 experimental groups. We removed 483 poorly expressed ORFs.

856 **Fig S9. Samples cluster by strain and growth conditions.** PCA plot displaying the filtered
857 CPM from all 12 experimental groups.

858 **Table S1. DEseq2 results comparing YPD *dhh1Δ/Δ* vs. YPD WT for Fig 6A.** Exponentially
859 growing *dhh1Δ/Δ* and WT SC5314 yeast cells in YPD at 30°C. RNA extraction performed in
860 triplicate from three separate samples.

861 **Table S2. DEseq2 results comparing RPMI *dhh1Δ/Δ* vs. RPMI WT for Fig 6C***.* *dhh1Δ/Δ* and
862 WT SC5314 grown under physiologically relevant filamentation conditions (RPMI + 10% serum
863 at 37°C) for 4 hours. RNA extraction performed in triplicate from three separate samples.

864 **Table S3. DEseq2 results comparing RPMI WT vs YPD WT for Fig 7A.** WT SC5314 yeast
865 cells in YPD at 30°C and WT SC5314 grown under physiologically relevant filamentation
866 conditions (RPMI + 10% serum at 37°C) for 4 hours. RNA extraction performed in triplicate from
867 three separate samples.

868 **Table S4. DEseq2 results comparing RPMI *dhh1Δ/Δ* vs YPD *dhh1Δ/Δ* for Fig 7D.** *dhh1Δ/Δ*
869 yeast cells in YPD at 30°C and *dhh1Δ/Δ* grown under physiologically relevant filamentation

870 conditions (RPMI + 10% serum at 37°C) for 4 hours. RNA extraction performed in triplicate from

871 three separate samples.

872 **Table S5. List of strains, plasmids, and primers used in this study.** This table includes

873 relevant information concerning our strain generation and validation.